Mon. Not. R. Astron. Soc. **373,** 1227–1234 (2006) doi:10.1111/j.1365-2966.2006.11104.x

Stable satellites around extrasolar giant planets

R. C. Domingos,[1,2]★ O. C. Winter[1,2] and T. Yokoyama[1,3]

[1] *INPE - Programa de Pós Graduação em Engenharia e Tecnologias Espaciais, São José dos Campos, CP 515, CEP 12201-970, Brazil*
[2] *UNESP - Grupo de Dinâmica Orbital e Planetologia, Guaratinguetá, CP 205, CEP 12.516-410, Brazil*
[3] *UNESP - IGCE DEMAC, Rio Claro, CP 178, CEP 13.500-970, Brazil*

Accepted 2006 September 24. Received 2006 September 19; in original form 2006 June 14

ABSTRACT

In this work, we study the stability of hypothetical satellites of extrasolar planets. Through numerical simulations of the restricted elliptic three-body problem we found the borders of the stable regions around the secondary body. From the empirical results, we derived analytical expressions of the critical semimajor axis beyond which the satellites would not remain stable. The expressions are given as a function of the eccentricities of the planet, $e_{\rm P}$, and of the satellite, $e_{\rm sat}$. In the case of prograde satellites, the critical semimajor axis, in the units of Hill's radius, is given by $a_{\rm E} \approx 0.4895\ (1.0000 - 1.0305 e_{\rm P} - 0.2738 e_{\rm sat})$. In the case of retrograde satellites, it is given by $a_{\rm E} \approx 0.9309\ (1.0000 - 1.0764 e_{\rm P} - 0.9812 e_{\rm sat})$. We also computed the satellite stability region ($a_{\rm E}$) for a set of extrasolar planets. The results indicate that extrasolar planets in the habitable zone could harbour the Earth-like satellites.

Key words: celestial mechanics – planets and satellites: general – planetary systems.

1 INTRODUCTION

In the last years the discovery of planets in other Solar systems led to the question of whether these planets also have satellites. A remarkable feature of the giant planets of our Solar system is the general architecture in the population of their satellites: all of the giant planets have at least two distinct groups. Very close to the planet, there is a class of regular satellites (almost planar and circular). The second group is formed with small objects with high eccentricity and high inclination (usually in retrograde orbits). However, it is important to emphasize that all of the giant planets of our Solar system are rather far from the Sun (the closest is the Jupiter which is about 5.2 au away). Now, the question that arises is related to the stability or the possibility that a giant planet hosts a satellite, in the case that the planet is closer to the star. For the time being, a significant number of extrasolar planets were discovered very near to the star, several have pericentre smaller than 0.1 au. The orbits of these planets are almost circular. In opposition, there are some interesting cases where for larger semimajor axis, the eccentricities tend to be high, reaching a maximum of about 0.93. The planet mass is a function of the inclination ($i_{\rm P}$) of the orbit with the observer's line of sight and it is given in terms of the Jupiter mass by $M_{\rm J}$ sin $i_{\rm P}$.

The question of habitability in these extrasolar systems is a relevant issue. The Earth-like life is unlikely in these planets but rocky moons orbiting these planets could be habitable if the planet–moon system orbits the parent star within the so-called 'habitable zone', where life-supporting liquid water could be present (Williams, Kasting & Wade 1997).

Up to now, satellites of extrasolar planets were not detected. This is mainly due to the instrumental limitations and the adopted techniques. Several missions to search for extrasolar planet transits by high-precision space-based photometry are in under development and will have the capacity to detect flux variations at the 10^{-5} level (Hui & Seager 2002), that might be enough to detect some large satellites (Sartoretti & Schneider 1999).

As mentioned before, due to the characteristics of the detected planetary systems it is natural to question which would be the possible conditions for the formation of satellites in this context. An aspect that can be explored without the need of having a closed theory on the formation of satellites is the stability of satellites in the advanced stages of evolution, where the formation process is almost ended. In this context, the main goal of this work is to infer the stability regions of prograde and retrograde orbits of planetary satellites in the presence of the star gravitational field.

Very roughly speaking, the idea of the limit of stability can be posed in the following way: consider a particle orbiting a planet which in its turn orbits a star. If the particle is far enough from the planet, the perturbation caused by the star becomes so important, that the particle cannot remain orbiting the planet. The region around the planet where the particle can survive, for any initial condition, for any time, defines a stable boundary and therefore a limit of stability. There is a close relation between the escape and the stability boundary of satellites. We can determine this limit by looking at the outermost regions where the majority of orbits are stable. This limit of stability depends on whether the satellite orbit is prograde (angular velocity is in the same sense as the planet) or

★E-mail: rcassia@feg.unesp.br

retrograde (angular velocity is in the opposite sense). It is important to note that the border of the stable region is complex and possibly fractal.

There is a series of papers about the escape and the capture of planetary satellites (for example: Heppenheimer & Porco 1977; Huang & Innanen 1983; Brunini 1996; Vieira Neto & Winter 2001a,b). Hunter (1967) obtained boundaries between escape and stable orbits for eccentric satellites under influence of Jupiter and the Sun. Hunter found that the lifetime of a satellite was decreased as the eccentricity was increased. He also deduced that for prograde orbits the stability region corresponds to approximately 0.44 of the radius of the planet's Hill's sphere – $R_{\mathrm{Hill}} = (\mu/3)^{\frac{1}{3}}$, where μ is the mass ratio of planet/star. For retrograde satellite orbits the stability region found was 0.74 R_{Hill}. Hénon (1969) found that a family of simple periodic retrograde orbits is stable even when the distance from the smaller primary tends to infinity, and around this family there is a stability region. This is valid for all mass ratios smaller than 0.0477 (Hénon & Guyot 1970).

An extensive literature is dedicated to the question of analytical stability boundary. Many estimates for circular orbits have been made from considering zero-velocity curves or equating forces in a rotating frame (Szebehely 1978; Innanen 1979; Graziani & Black 1981; Pendleton & Black 1983; Hamilton & Burns 1991, 1992; Donnison & Mikulskis 1994; and others). In these studies, it has been shown that the retrograde orbits are stable at longer distances than direct orbits.

Holman & Wiegert (1999) investigated in what regions around a binary system, a body can orbit the centre of mass of the stars (or one of the stars) for long time. These authors investigated numerically, the orbital stability in the frame of the elliptic-restricted three-body problem. They considered a circular orbit for the third body. Empirical expressions that give the critical semimajor axis (a_c) as a function of the eccentricity (e) and mass ratio (μ) of the binaries are developed. Such expressions are derived for binary systems with $0.0 \leqslant e \leqslant 0.8$ and mass ratio $0.1 \leqslant \mu \leqslant 0.9$. The formula for bodies orbiting one of the stars is not predicted for the case $\mu \to 0$; however, simulations at $e = 0$ and in the range $0.9 \leqslant \mu \leqslant 1.0$ were made and a plot of a_c as a function of μ is given.

We noted in the literature some limitations. First, the results of the stability boundary of satellites have been done for the cases of planets with circular orbits. Secondly, there is not a general expression for the stability boundary that explicitly included the eccentricities of the planet and the satellite. Thirdly, the numerical results have been limited to fairly short integrations.

In this work, we simulated only the case $\mu = 10^{-3}$ and it differs from Holman & Wiegert's work in the sense that here we consider a wide range of eccentricities of both bodies, that is, the secondary and also the particle's eccentricity. Moreover, from our results we derive an expression for the critical stable semimajor axis of the particle as a function of the secondary mass and of eccentricities of both bodies. Our purpose is to derive the empirical expression of stability boundary for prograde and retrograde orbits. These expressions can be more directly applicable to current searches of satellites in extrasolar planetary systems. It is our hope that these results can be used as a guide in selecting a sample of suitable candidates for a survey of satellites.

This paper is structured as follows. In Section 2, we present the numerical approach adopted and give the results found. Section 3 is devoted to the analysis of the numerical results. In Section 4, we discuss the implications of our results for the existence of satellites around extrasolar planets. Our conclusions are presented in Section 5.

2 NUMERICAL SIMULATIONS

In this study we numerically investigate the orbital stability within the elliptic-restricted three-body problem, Star-planet–satellite. The numerical code is based on the Gauss–Radau integrator (Everhart 1985) and has been fully tested (Vieira Neto & Winter 2001a).

The satellite is modelled as a test particle moving in the gravitational fields of the star and the planet on a fixed eccentric orbit about the star. In agreement with Holman & Wiegert (1999), in the systems with high mass ratio, the stability limit (or the critical semimajor axis) of a body in a circular orbit is $a \propto f\, R_{\mathrm{Hill}}$, where f is a constant.

In this work the numeric estimates of the value of f is obtained considering a grid of initial conditions for the satellites with the following initial conditions for the planet: semimajor axis (a_{p}) 0.1 au, eccentricity e_{p} from 0.0 to 0.9 with $\Delta e_{\mathrm{P}} = 0.1$. The initial angular elements true anomaly f and the longitude of pericentre ϖ are taken to be zero and the inclination is 0° for the prograde case and 180° for the retrograde one.

For the hypothetical satellites, we take the initial semimajor axis (a_{sat}) from 1.1 to $40R_{\mathrm{P}}$ (R_{P} is the Jupiter's radius) and initial eccentricity (e_{sat}) from 0.0 to 0.5. Prograde satellites assumed $\Delta a_{\mathrm{sat}} = 0.1R_{\mathrm{P}}$ and $\Delta e_{\mathrm{sat}} = 0.01$. Retrograde satellites assumed $\Delta a_{\mathrm{sat}} = 0.2R_{\mathrm{P}}$ and $\Delta e_{\mathrm{sat}} = 0.025$. The retrograde orbits are stable at larger semimajor axes than the prograde orbits (Hamilton & Krivov 1997), so we reduced the grid for the initial conditions (a_{sat}, e_{sat}) to test the retrograde orbits. We justify our choice for to reduce the amount of computer time.

The numeric simulations were made for an interval of 10^4 planet's orbital periods. The integration was interrupted whenever one of the situations appeared: collision between the satellite and the planet, the satellite collided with the Star or the satellite's planetocentric energy became positive (escape) (Vieira Neto, Winter & Melo 2005). The initial conditions of the survived satellites for full integration time were considered stable. Thus, each point in the figures corresponds to one trajectory.

2.1 Prograde case

The numerical results for the prograde case are presented in Figs 1 and 2. There we illustrate a_{sat} up to $20R_{\mathrm{P}}$ for better graphic visibility

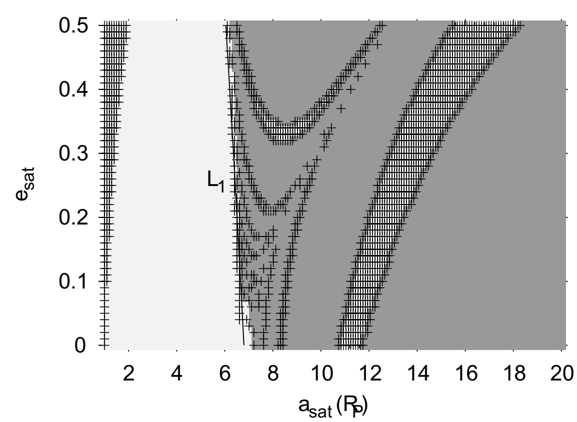

Figure 1. Regions of stability of hypothetical prograde satellites in the space of initial conditions a_{sat} versus e_{sat}, for a planet in a circular orbit. The white region corresponds to the stable region. The outer border of this region corresponds to the zero-velocity curve associated to L_1. The grey colour indicates the unstable regions. The symbol + refers to the collision of the satellite.

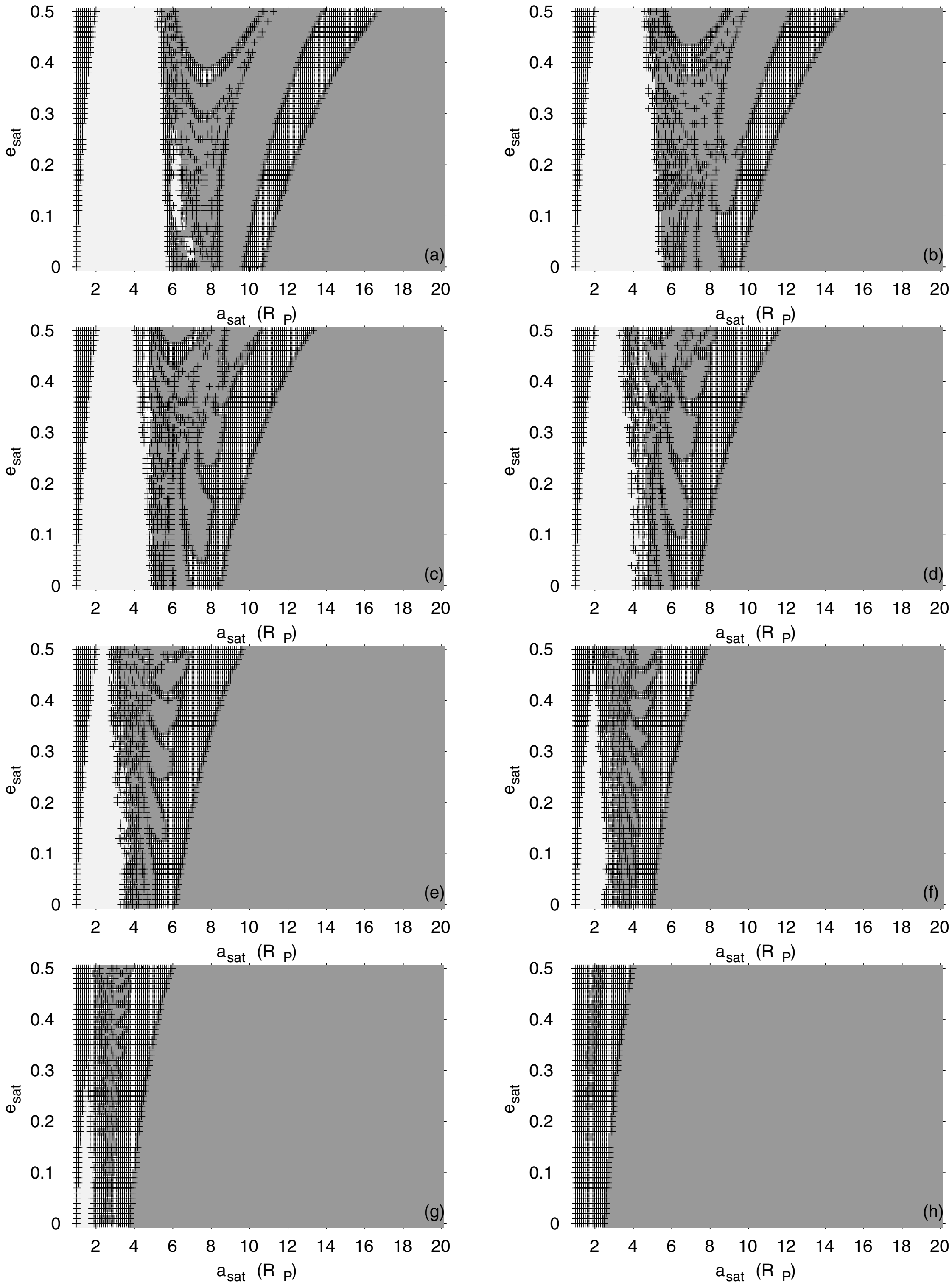

Figure 2. Regions of stability of hypothetical prograde satellites in the space of initial conditions a_{sat} versus e_{sat}. In each plot the planet has a given eccentricity: (a) $e_P = 0.1$; (b) $e_P = 0.2$; (c) $e_P = 0.3$; (d) $e_P = 0.4$; (e) $e_P = 0.5$; (f) $e_P = 0.6$; (g) $e_P = 0.7$ and (h) $e_P = 0.8$. The white regions correspond to stable regions. The grey colour indicates the unstable regions. The symbol + refers to the collision of the satellite.

of the stable region. In Fig. 1, the orbit of the planet was assumed to be circular. The line at the border to the right of the white region corresponds to the zero-velocity curve associated to L_1. One of the important features presented in the results was that usually satellites escape in a maximum time of 320 orbital periods of the planet. In agreement with Rabl & Dvorak (1988) and Holman & Wiegert (1999), an integration time of approximately 300 primary's orbital periods would be enough to determine the gross stability boundary.

In our simulations, it is noticed that the stability region extends to about seven planetary radius what corresponds to approximately

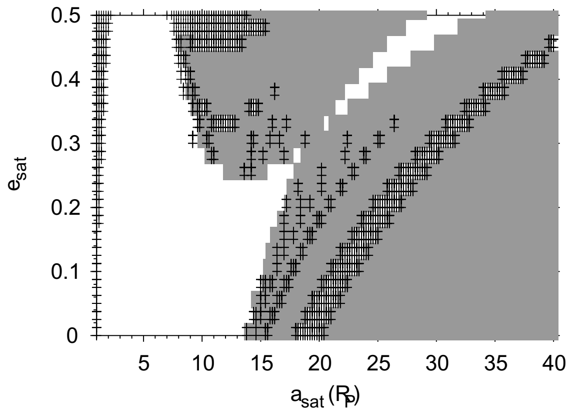

Figure 3. Regions of stability of hypothetical retrograde satellites in the space of initial conditions $a_{\rm sat}$ versus $e_{\rm sat}$, for a planet in a circular orbit. The white region corresponds to the stable region. The grey colour indicates the unstable regions. The symbol + refers to collision of the satellite.

half of $R_{\rm Hill}$. Therefore, the stability region limit is approximately given by $a = R_{\rm Hill}/2$ for $e_{\rm P} = e_{\rm sat} = 0$.

In Fig. 2, we present the results for elliptic cases where $e_{\rm P}$ assumes values from 0.1 to 0.8 with $\Delta e_{\rm P} = 0.1$. In such cases the stability region reduces with the increase of the planet's eccentricity, as expected.

Planets with the same initial semimajor axis but with a larger eccentricity have a smaller stability region. This is not perhaps surprising because a planet (or a satellite) with a larger orbital eccentricity is able to wander further from a star (or a planet) than one with a smaller one, and will therefore suffer larger perturbations from the star (or the planet). Our results suggest that for $e_{\rm P} > 0.8$ the stability region tends to disappear.

2.2 Retrograde case

The numerical results for the retrograde case are presented in Figs 3 and 4. In Fig. 3, the orbit of the planet was assumed to be circular. Usually satellites escape or collide with the planet in less than 200 orbital periods of the planet. Therefore, satellites that survive for more than 200 orbital periods are stable. The results lead to the same conclusions regarding the greater stability region for circular orbits (Fig. 3). It is important to note that in the retrograde case there are stability regions even outside the zero-velocity curve associated to L_1. In the case of satellites in circular orbits, we have found that the stability region extends to about 13.6 planetary radius. Therefore, the stability region limit is approximately given by $a = R_{\rm Hill}$ for $e_{\rm P} = e_{\rm sat} = 0$. The retrograde orbits are stable out for higher values of the eccentricity and to considerably greater distances from the planet than the prograde orbits. These stable regions are due to the quasi-periodic orbits associated to the periodic orbits of family 'F' (Vieira Neto & Winter 2001b).

In Fig. 4, we present the results for elliptic cases where $e_{\rm P}$ assumes values from 0.1 to 0.8 with $\Delta e_{\rm P} = 0.1$. In such cases the stability region reduces with the increase of $e_{\rm P}$, as expected. The quasi-periodic orbits, associated to the periodic orbits of family 'F', are destroyed with the increase of $e_{\rm P}$. Our results suggest that for $e_{\rm P} > 0.9$ the stability region tends to disappear.

3 ANALYSIS OF THE RESULTS

According to these results, the stability boundary has two borders: one internal and other external. We noted that there are escape and collision orbits close to the borders. As expected, these borders have dependence on $e_{\rm P}$ and $e_{\rm sat}$. In Fig. 5, we present a sketch showing the dependence of $e_{\rm sat}$ on $a_{\rm sat}$ illustrating the stability and instability regions of the satellites. The white area corresponds to the stability region, delimited by what we called internal ($a_{\rm I}$) and external ($a_{\rm E}$) critical semimajor axis. The grey area corresponds to escape or collision of satellites.

It can be seen that the inner border separates the collision and stable regions. In this case, what dominates the collision process is the distance of the satellite to the planet. Satellites suffer a small gravitational perturbation of the star and they are subjected to a relatively larger gravitational influence of the planet. The usual effects of such perturbation can be seen from collision trajectories.

Since the relative strengths of perturbations change with separations, trajectories of the satellites have quite different characteristics depending on their distances from the planet. Satellites have stable orbits since the planet's gravity dominates all perturbations. When the distance is increased, the star's perturbation becomes so large that in such region the forces from the star and planet are comparable. Then, the escape or the collision of the satellite with the planet can occur. We call 'stability boundary' or external critical semimajor axis ($a_{\rm E}$), the 'limit' between the regions of stable orbits and that of the collision/escape orbits.

Our results show differences between the value of $a_{\rm E}$ for the prograde and retrograde cases. For the retrograde case, a combination of increased values of $a_{\rm sat}$ and $e_{\rm sat}$ produces a stability region beyond that for prograde orbits. Also, after a certain value of $a_{\rm sat}$ it appears as a stable region of quasi-periodic orbits associated to the periodic orbits of family 'F'.

Following the idea that there are critical distances of the planet, given by $a_{\rm I}$ and $a_{\rm E}$, beyond which the satellite will collide or escape, we determined such boundaries from the results of our simulations. For each pair of values of $e_{\rm P}$ and $e_{\rm sat}$ the value of $a_{\rm I}$ and $a_{\rm E}$ are measured. From these numbers, empirical expressions that give the critical semimajor axis as functions of $e_{\rm P}$ and $e_{\rm sat}$ are derived. The $a_{\rm E}$ is the most important result because within this stability boundary it is expected that there can exist stable satellite orbits around the planet.

For the prograde case, the results of approximately 50 points for each value of $e_{\rm P}$ are used to establish an analytical expression for $a_{\rm I}$ and $a_{\rm E}$ as functions of $e_{\rm P}$ and $e_{\rm sat}$. For the retrograde case, the expression for $a_{\rm I}$ was derived from about seven points for each value of $e_{\rm P}$. The expression for $a_{\rm E}$ was obtained using two points for each value of $e_{\rm P}$. In this sense, we choose the first ($e_{\rm sat} = 0$) and the last (highest $e_{\rm sat}$) value for $a_{\rm E}$ on the external border of the regions. The points considered on the borders of regions do not included the regions of quasi-periodic orbits associated to the periodic orbits of family 'F'. A fit using an implementation of the non-linear least-squares through a Marquardt–Levenberg algorithm to the data yields for the prograde case

$$a_{\rm I} = (1.0891 \pm 0.0049) + (0.4576 \pm 0.0472)e_{\rm sat} + (2.9559 \pm 0.0932)e_{\rm sat}^2, \quad (1)$$

$$a_{\rm E} = (7.0051 \pm 0.0363) - (1.9180 \pm 0.0687)e_{\rm sat} - (7.2189 \pm 0.0543)e_{\rm P} \quad (2)$$

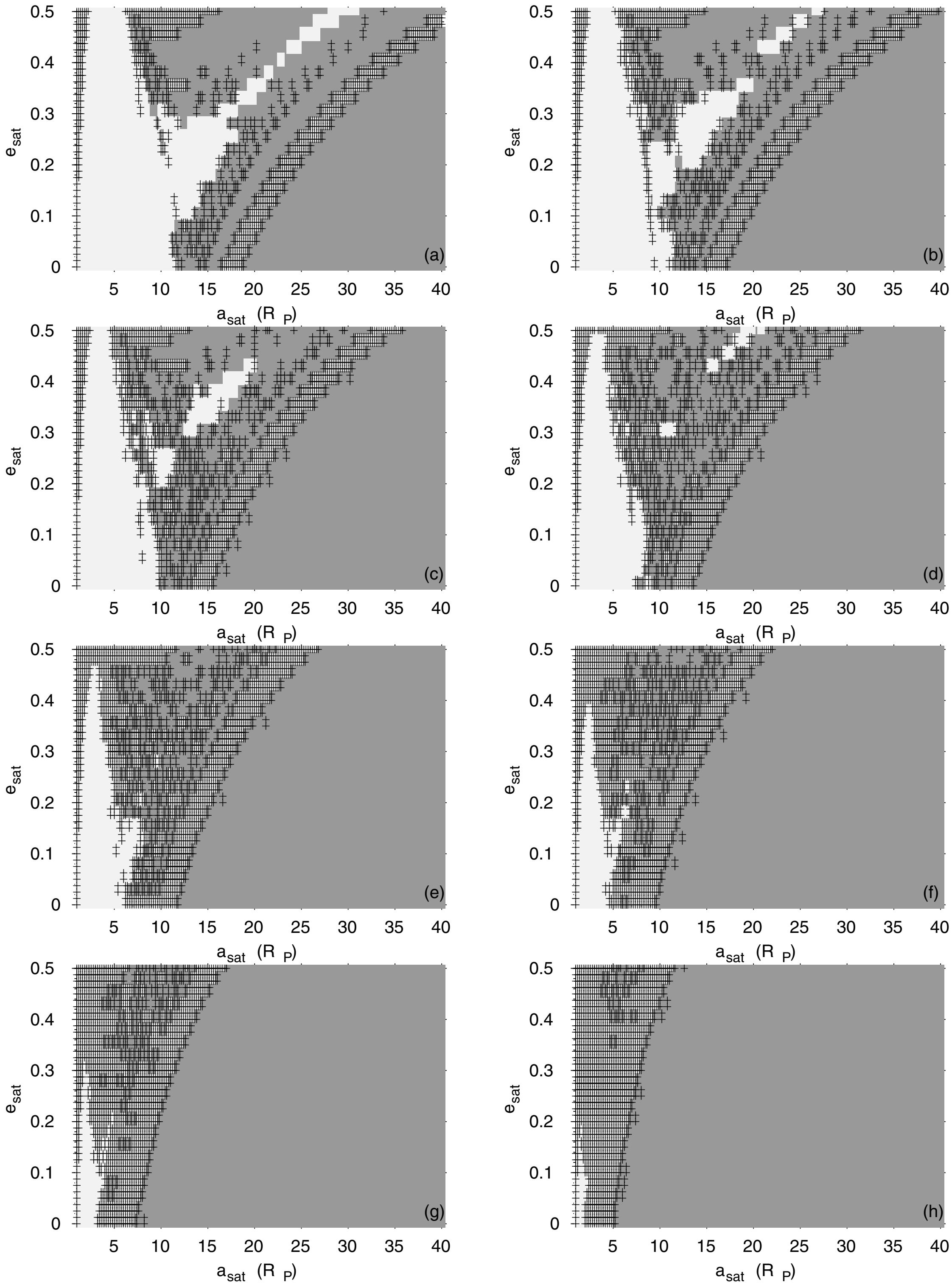

Figure 4. Regions of stability of hypothetical retrograde satellites in the space of initial conditions a_{sat} versus e_{sat}. In each plot the planet has a given eccentricity: (a) $e_{\mathrm{P}} = 0.1$; (b) $e_{\mathrm{P}} = 0.2$; (c) $e_{\mathrm{P}} = 0.3$; (d) $e_{\mathrm{P}} = 0.4$; (e) $e_{\mathrm{P}} = 0.5$; (f) $e_{\mathrm{P}} = 0.6$; (g) $e_{\mathrm{P}} = 0.7$ and (h) $e_{\mathrm{P}} = 0.8$. The white regions correspond to stable regions. The grey colour indicates the unstable regions. The symbol + refers to the collision of the satellite.

and for the retrograde case

$$a_{\mathrm{I}} = (1.1271 \pm 0.1367) + (5.4003 \pm 0.2289)e_{\mathrm{sat}}^2, \quad (3)$$

$$\begin{aligned} a_{\mathrm{E}} = {} & (13.3214 \pm 0.4974) - (14.3395 \pm 0.6791)e_{\mathrm{P}} \\ & - (13.0716 \pm 1.177)e_{\mathrm{sat}} + (12.5821 \pm 1.877)e_{\mathrm{P}}e_{\mathrm{sat}}. \end{aligned} \quad (4)$$

These expressions are given in terms of the planet's radius units. Each coefficient is listed along with its formal uncertainty.

Following the idea that the stability region is proportional to the size of the Hill's sphere of the planet, our results can be considered for other values of semimajor axis (a_{P}) and the masses of the planet

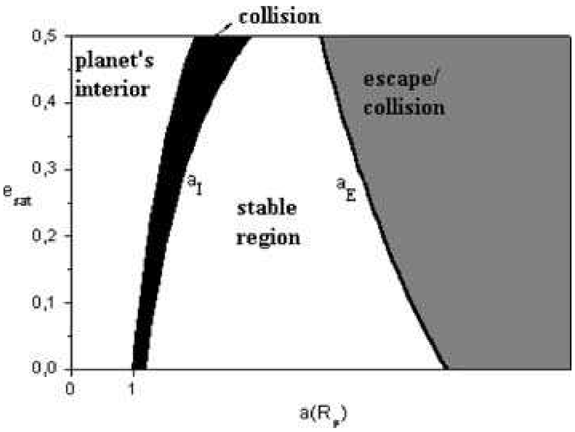

Figure 5. Sketch illustrating the stability and instability regions of prograde satellites in the initial conditions space, $a_{\rm sat} \times e_{\rm sat}$. The stable region is delimited by the internal ($a_{\rm I}$) and external ($a_{\rm E}$) critical semimajor axes. The left-hand border of the black region is determined by $a(1 - e_{\rm sat}) = R_{\rm P}$.

and the star ($M_{\rm P}$ and $M_\star$). The difference of the results will be just scalefactors (Hamilton & Burns 1991). Therefore, the expressions for $a_{\rm E}$ can be written in terms of the Hill's radius. We found for the prograde case (equation 2),

$$a_{\rm E} \approx 0.4895\ (1.0000 - 1.0305 e_{\rm P} - 0.2738 e_{\rm sat}) \tag{5}$$

and for the retrograde case (equation 4)

$$a_{\rm E} \approx 0.9309\ (1.0000 - 1.0764 e_{\rm P} - 0.9812 e_{\rm sat} + 0.9446 e_{\rm P} e_{\rm sat}). \tag{6}$$

Analysing these expressions, it can be noted that the values of $a_{\rm I}$ do not depend on the $e_{\rm P}$ value and they can be regarded as empirical planet's collision lines as it is shown in Figs 5 and 6. In this two cases the numerical estimates (equations 1 and 3) and calculated values (planet's collision line) are very close. Undoubtedly, there exists a strong dependence on the satellite eccentricity which is physically clear from the fact that the gravitational perturbation of the planet on the satellite increases significantly with $e_{\rm sat}$.

For the external semimajor axis, we can see immediately the decrease of $a_{\rm E}$ with $e_{\rm P}$, which can be explained by the decrease of the minimum distance between the primaries. Thus, the perturbations felt by an orbiting satellite are maximum when the planet is near the pericentre of its orbit. In general, therefore, satellites would be expected to escape during the movement of the planet through its pericentre. Hamilton & Burns (1992) studied the forces' components acting on the problem of initially elliptic orbits. They concluded that the stability region scales roughly as the size of the Hill's sphere calculated at the planet's pericentre. Analysing equations (5) and (6) we have that for $e_{\rm P} = e_{\rm sat} = 0$ $a_{\rm E} \approx R_{\rm Hill}/2$ and $a_{\rm E} \approx R_{\rm Hill}$, respectively. When $e_{\rm P}$ is different from zero, $a_{\rm E}$ decreases by a scalefactor of approximately $(1 - e_{\rm P})$, i.e., the relation $a_{\rm E} \propto f R_{\rm Hill}$, is still valid, but now $R_{\rm Hill}$ will be computed at the planet's pericentre. It is also interesting to note that for retrograde orbits there is a stronger dependence on $e_{\rm sat}$ than for the prograde orbits. With the increase of the value of $e_{\rm sat}$ the size of the stable region of retrograde orbits reduces more than that for prograde orbits.

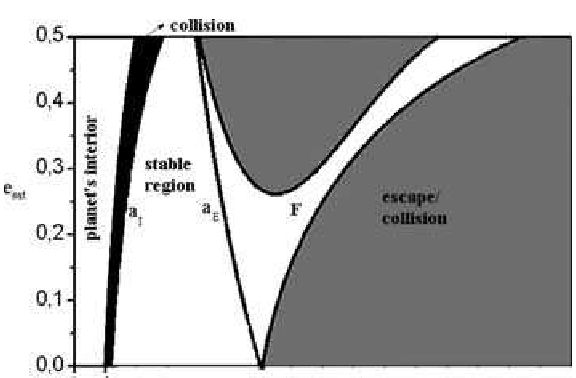

Figure 6. Sketch illustrating the stability and instability regions of retrograde satellites in the initial conditions space, $a_{\rm sat} \times e_{\rm sat}$. The stable region is delimited by the internal ($a_{\rm I}$) and external ($a_{\rm E}$) critical semimajor axes. The white region denoted by the letter 'F' corresponds to the stable region associated to the family of periodic orbits named F. The left-hand border of the black region is determined by $a(1 - e_{\rm sat}) = R_{\rm P}$.

4 EXTRASOLAR PLANETS' SATELLITES

For planets orbiting close to the star, the tidal effect induced by the star on the planet slows down the planet's rotation. Then, the resulting tidal effect of the planet on a satellite makes it migrate internally towards the planet. Eventually these satellites collide with the planet or are broken up once they migrate inside the Roche limit. The Roche limit for fluid satellite is given by $R_{\rm Roche} = 2.46 R_{\rm P}$ (Chandrasekhar 1968). Therefore, the satellite of a planet with critical semimajor axis smaller than $2.46 R_{\rm P}$ would have to be small (broken pieces).

Barnes & O'Brien (2002) presented a study on the stability of satellites in the circular orbits around extrasolar planets that are close to their stars. Following that, we describe and adopt the analytical treatment that they used in order to estimate the superior limit of the mass for primordial satellites that could have survived to these tidal effects.

There are three possible outcomes of tidal evolution in planet–satellite systems: (i) the orbit may move outward towards escape; (ii) the satellite's orbital and the planet's spin periods may approach stable synchronism and (iii) the satellite orbit may decay inward towards the planet. In this study, we considered only the third possibility. Considering that the lifetime T of a satellite can be given by the time needed for its orbit to cross the region between the critical semimajor axis, $a_{\rm E}$, and the surface of the planet, $R_{\rm P}$, we have that (Murray & Dermott 1999)

$$T = \frac{2}{13}\left(a_{\rm E}^{13/2} - R_{\rm P}^{13/2}\right)\frac{Q_{\rm P}}{3 k_{2P} M_{\rm sat} R_{\rm P}^5}\sqrt{\frac{M_{\rm P}}{G}}, \tag{7}$$

where $Q_{\rm P}$ is the tidal dissipation factor, k_{2P} is the Love number, G is the gravitational constant and $M_{\rm sat}$ is the satellite mass. Since $R_{\rm P} \ll a_{\rm E}$, the term $R_{\rm P}^{13/2}$ in parentheses can be neglected. Using $a_{\rm E} = f R_{\rm Hill}$ and T as the age of the star, the maximum satellite mass is given by

$$M_{\rm sat} = \frac{2}{13}\,(f R_{\rm Hill})^{13/2}\,\frac{Q_{\rm P}}{3 k_{2P} T R_{\rm P}^5}\sqrt{\frac{M_{\rm P}}{G}}. \tag{8}$$

Barnes & O'Brien (2002) estimated the maximum mass of the prograde satellites in a circular orbit around a set of extrasolar planets with $a_{\rm P} < 0.3$ au. For the mass ratio $M_{\rm P}/M_{\rm star} = M_{\rm J}/{\rm M}_\odot$ they used $f = 0.36$, from Holman & Wiegert (1999). They considered only planets with near circular orbits because $a_{\rm E}$ had not been found for eccentric orbits.

From equation (5) we have that $f = 0.4895$ when $e_{\rm P} = e_{\rm sat} = 0$, which is significatively larger than that found by Holman & Wiegert (1999). Our results were also generated for different values of $e_{\rm P}$.

Table 1. External critical semimajor axis, a_E, and the maximum satellite mass for a selection of extrasolar planets with $a_P \leqslant 1.1$ au. The computation of a_E was made using equation (5), for prograde satellites with a circular orbit ($e_{sat} = 0$), and the results are given in a planetary radius, R_P, assuming that the planet has the same density as that of the Jupiter.

Star	$M_\star (M_\odot)$	$M_P \sin i_P$ (M_J)	a_P (au)	e_P	a_E (R_P)	M_{sat} ($M_\oplus$)
HD73256	1.05	1.85	0.037	0.04	2.35	2.4×10^{-5}
HD179949	1.24	0.98	0.040	0.00	2.61	1.9×10^{-5}
HD46375	1.00	0.25	0.041	0.04	2.64	6.9×10^{-6}
HD187123	1.06	0.54	0.042	0.01	2.83	1.9×10^{-5}
BD-103166	1.10	0.48	0.046	0.05	2.81	2.1×10^{-5}
HD209458	1.05	0.63	0.046	0.02	3.04	3.8×10^{-5}
Tau Boo	1.30	4.14	0.047	0.04	2.78	1.6×10^{-4}
HD75289	1.05	0.46	0.047	0.01	3.18	3.4×10^{-5}
HD76700	1.00	0.19	0.049	0.00	3.43	2.2×10^{-5}
51 Peg	1.00	0.46	0.052	0.01	3.57	7.3×10^{-5}
HD49674	1.00	0.12	0.057	0.00	3.99	3.7×10^{-5}
HD168746	0.92	0.24	0.066	0.00	4.76	2.3×10^{-4}
HD68988	1.20	1.90	0.071	0.14	3.45	2.8×10^{-4}
HD217107	0.98	1.29	0.072	0.14	3.74	6.9×10^{-4}
HD162020	0.70	14.40	0.074	0.28	2.99	5.8×10^{-3}
HD130322	0.79	1.15	0.092	0.05	6.28	9.5×10^{-3}
HD108147	1.20	0.40	0.104	0.40	2.42	1.3×10^{-4}
GJ86	0.79	4.23	0.117	0.04	8.16	1.8×10^{-1}
HD195019	1.02	3.55	0.136	0.02	9.09	2.6×10^{-1}
HD6434	1.00	0.48	0.154	0.30	5.22	8.6×10^{-3}
HD192263	0.79	0.75	0.150	0.03	10.69	1.7×10^{-1}
Rho Crb	0.95	0.99	0.224	0.07	13.78	1.5
HD3651	0.79	0.20	0.284	0.63	2.79	3.9×10^{-3}
HD121504	1.00	0.89	0.317	0.13	16.74	7.6
HD178911	0.90	6.46	0.326	0.14	17.41	7.7×10^{1}
HD16141	1.00	0.22	0.351	0.21	15.23	1.9×10^{1}
HD114762	0.82	10.96	0.351	0.33	11.62	4.7×10^{1}
HD80606	0.90	3.43	0.438	0.93	0.09	8.1×10^{-7}
HD216770	0.90	0.70	0.460	0.32	15.22	1.6×10^{1}
70 Vir	1.10	7.41	0.482	0.40	11.54	6.3×10^{1}
HD52265	1.13	1.14	0.493	0.29	16.51	1.3×10^{1}
HD1237	0.96	3.45	0.505	0.51	8.34	5.3×10^{1}
HD73526	1.02	3.63	0.647	0.52	10.03	9.4×10^{2}
HD8574	1.10	2.04	0.770	0.31	24.55	9.4×10^{2}
HD40979	1.08	3.16	0.818	0.26	30.27	1.7×10^{4}
HD150706	0.98	1.00	0.820	0.38	21.82	4.3×10^{2}
HD134987	1.05	1.63	0.821	0.37	22.06	6.8×10^{2}
HD169830	1.40	2.95	0.823	0.34	22.10	9.2×10^{2}
HD202206	0.90	17.50	0.830	0.43	19.12	5.5×10^{3}
HD89744	1.40	7.17	0.883	0.70	4.62	1.4×10^{1}
HD17051	1.03	1.94	0.910	0.24	36.12	5.9×10^{3}
HD92788	1.06	3.88	0.969	0.28	34.11	1.2×10^{4}
HD142	1.10	1.36	0.980	0.37	25.93	1.6×10^{3}
HD128311	0.80	2.63	1.010	0.21	47.20	3.5×10^{4}
HD28185	0.99	5.70	1.030	0.07	62.49	1.6×10^{5}
HD108874	1.00	1.65	1.070	0.20	47.62	2.2×10^{4}
HD142415	1.03	1.73	1.070	0.50	18.00	8.6×10^{2}
HD4203	1.06	1.64	1.090	0.53	15.98	5.6×10^{2}
HD177830	1.17	1.24	1.100	0.40	12.95	2.0×10^{3}

In the case of prograde satellites in circular orbits we have

$$f(e_P) = 0.4895(1 - 1.0305 e_P). \tag{9}$$

In Table 1, the external critical semimajor axis for prograde satellites in circular orbits, a_E (equation 5) and the maximum satellite mass (equation 9) for a selection of extrasolar planets (http://exoplanets.org) are given. The tidal effects will not force planets to be synchronous if they have semimajor axis larger than 0.1 au. Just for comparison, we considered a set of extrasolar planets with $a_P \leqslant 1.1$ au.

Analysing these results we have found that even planets that are very close to the star, $a_p < 0.1$ au, can harbour a satellite with mass close to that of our Moon. We also noted that the Rho Crb's planet, which has $a_P = 0.224$ au, could have a satellite with the Earth's mass. For the planets in the habitable zone ($0.9 < a_P < 1.1$ au), all the planets studied have a large stable region and could easily support the Earth-like satellites.

A comparison with the results from Barnes & O'Brien (2002) shows that, in general, the maximum satellite mass is one order of magnitude higher than the values they found. That is a direct consequence of the value of f used by them and the one we derived from our numerical simulations.

5 CONCLUSIONS

In this work, we have derived empirical expressions for the critical semimajor axis of the borders of the satellite stable region for a planet around a star. The expressions derived are given in terms of the Hill's radius and as a function of the eccentricities of the planet and the satellite. That is a significant step forward with respect to previous results. Our results also indicate that extrasolar planets in the habitable zone could harbour the Earth-like satellites.

ACKNOWLEDGMENTS

The authors thank J. W. Barnes and D. P. O'Brien for providing information about their results and P. A. Wiegert for his suggestions. This work was funded by Capes, CNPq and Fapesp. This support is gratefully acknowledged.

REFERENCES

Barnes J. W., O'Brien D. P., 2002, ApJ, 575, 1087
Brunini A., 1996, Cel. Mec. &Dyn. Ast., 64, 79
Chandrasekhar S., 1968, Ellipsoidal Figures of Equilibrium. Yale Univ. Press, New Haven, CT
Donnison J. R., Mikulskis D. F., 1994, MNRAS, 266, 25
Everhart E., 1985, in Carusi A., Valsecchi G. B., eds, Dynamics of Comets: Their origin and Evolution. D. Reidel Publishing Company, Dordrecht, p. 185
Graziani F., Black D. C., 1981, ApJ, 251, 337
Hamilton D. P., Burns J. A., 1991, Icarus, 92, 118
Hamilton D. P., Burns J. A., 1992, Icarus, 96, 43
Hamilton D. P., Krivov A. V., 1997, Icarus, 128, 241
Hénon M., 1969, A&A, 1, 223
Hénon M., Guyot M., 1970, in Giacaglia G. E. O., ed., Periodic Orbits, Stability and Resonances. D. Reidel Publishing Company, Dordrecht, p. 349
Heppenheimer T. A., Porco C., 1977, Icarus, 30, 385
Holman M. J., Wiegert P. A., 1999, AJ, 117, 621
Huang T. Y., Innanen K. A., 1983, AJ, 88, 1537
Hui L., Seager S., 2002, AJ, 572, 540
Hunter R. B., 1967, MNRAS, 136, 245
Innanen K. A., 1979, AJ, 84, 960
Murray C. D., Dermott S. F., 1999. Solar System Dynamics. Cambridge Univ. Press, Cambridge
Pendleton Y. J., Black D. C., 1983, AJ, 88, 1415
Rabl G., Dvorak R., 1988, A&A, 191, 385
Sartoretti P., Schneider J., 1999, A&AS, 134, 553
Szebehely I. R., 1978, Cel. Mec., 18, 383
Vieira Neto E., Winter O. C., 2001a, AJ, 122, 440
Vieira Neto E., Winter O. C., 2001b, A&A, 377, 1119
Vieira Neto E., Winter O. C., Melo C. F., 2005, in Knezevic Z., Milani A., eds, Dynamics of Populations of Planetary Systems. Cambridge Univ. Press, Cambridge, p. 439
Williams D. M., Kasting J. F., Wade R. A., 1997, Nat, 385, 234

This paper has been typeset from a TEX/LATEX file prepared by the author.